APL Materials

Reversible oxygen-induced *p*-doping of mixed-cation halide perovskites

Cite as: APL Mater. **9**, 081104 (2021); https://doi.org/10.1063/5.0056346
Submitted: 09 May 2021 • Accepted: 09 July 2021 • Published Online: 05 August 2021

Dongguen Shin, Fengshuo Zu and Norbert Koch

Reversible oxygen-induced *p*-doping of mixed-cation halide perovskites

Cite as: APL Mater. 9, 081104 (2021); doi: 10.1063/5.0056346
Submitted: 9 May 2021 • Accepted: 9 July 2021 •
Published Online: 5 August 2021

Dongguen Shin,[1] Fengshuo Zu,[1] and Norbert Koch[1,2,a)]

AFFILIATIONS

[1] Institut für Physik & IRIS Adelershof, Humboldt-Universität zu Berlin, 12489 Berlin, Germany
[2] Helmholtz-Zentrum Berlin für Materialien und Energie GmbH, 12489 Berlin, Germany

[a)] **Author to whom correspondence should be addressed:** norbert.koch@physik.hu-berlin.de

ABSTRACT

To fully unlock the potential of metal halide perovskites (MHPs) for use in optoelectronic devices, a comprehensive understanding of their electronic properties is in strong demand but presently lacking. This photoelectron spectroscopy study reveals that the thin films of three important mixed-cation/mixed-halide MHPs behave like intrinsic semiconductors with a very low defect concentration. The Fermi level position in the bandgap can be varied by almost 1 eV by choosing substrates of appropriate work function for samples that were handled under inert conditions. Upon oxygen exposure, two organic/inorganic-cation MHPs become strongly *p*-doped due to oxygen diffusion into the bulk, a process that is fully reversible when storing the samples in ultrahigh vacuum. In contrast, all-inorganic $CsPbI_{1.8}Br_{1.2}$ exhibits no electronic property changes upon oxygen exposure. Nonetheless, oxygen is found to effectively remove (light-induced) lead-related surface states of $CsPbI_{1.8}Br_{1.2}$.

I. INTRODUCTION

The successful application of metal halide perovskites (MHPs) in optoelectronic devices, most notably in solar cells, has sparked considerable interest also due to their fundamental material properties.[1–9] Accessing the electronic properties at the surface and device-relevant interfaces of MHPs not only allows for a better understanding of the material itself but also provides the insight needed for further enhancing device performance.[10–16] In this context, the electronic properties of MHPs have been intensively investigated; however, the pronounced variations of their apparent electronic characteristics have been reported, such as huge discrepancies in the Fermi level (E_F) position in the energy gap.[9,14,17–22] A probable underlying mechanism was reported recently for the prototypical methylammonium lead triiodide ($MAPbI_3$), where the reversible diffusion of oxygen into and out of thin films was revealed, which goes in hand with the reversible *p*-doping of $MAPbI_3$ by oxygen molecules.[23] In this study, it was further shown that $MAPbI_3$ thin films prepared under inert conditions and without oxygen exposure behave like an intrinsic, i.e., undoped, semiconductor. This was concluded from the observation in photoemission experiments that the E_F position followed the substrate work function (Φ_{sub}), unless Fermi level pinning at the conduction and valence band edges stopped the movement of E_F. After oxygen exposure, E_F was found pinned close to the valence band edge, independent of Φ_{sub}. Therefore, the appearance of $MAPbI_3$ as either *n*-type or *p*-type can result from varying Φ_{sub} values,[9,17,19,22] as long as weak interaction with the substrate prevails and defect-induced gap states play no major role.[23] It is thus of high relevance to answer the question whether the same phenomena also apply to the modern mixed-cation/mixed-halide MHPs, which feature improved device performance and lifetime.[24–27] In addition, different cation and halide combinations can affect the carrier density and doping[28] so that an extrapolation of results obtained for $MAPbI_3$ to modern MHPs should be substantiated by experiments. In this regard, it was reported that the E_F position in the gap can vary with Φ_{sub} by as much as 1.4 eV for bromide-only perovskites, i.e., $Cs_{0.05}FA_{0.85}MA_{0.1}PbBr_3$[17] and $CsPbBr_3$,[29] and by as much as 0.5 eV for a mixed-halide perovskite, i.e., $FA_{0.83}MA_{0.17}Pb(I_{0.83}Br_{0.17})_3$.[22] However, the Φ_{sub} range used in these studies was not sufficiently wide to investigate the full possible E_F-movement range, and a more comprehensive study is still missing. Moreover, the effect of oxygen exposure on the electronic properties and possibly associated *p*-type remains to be uncovered for the modern mixed MHPs.

In this work, we conducted a detailed study on the dependence of the thin film electronic properties of three mixed-cation/mixed-halide MHPs on Φ_{sub} and oxygen exposure via ultraviolet photoelectron spectroscopy (UPS). We found that the E_F value of all three perovskites, prepared in an inert gas atmosphere, does vary with Φ_{sub} seemingly from *n*-type to *p*-type, revealing the so-called "Z-curve" behavior.[30] This is characteristic of a very low intrinsic doping level and negligible surface state density of these MHPs.[23] In addition, controlled oxygen and vacuum exposure experiments show that oxygen exposure leads to the *p*-doping of $Cs_{0.05}(FA_{0.83}MA_{0.17})_{0.95}Pb(I_{0.83}Br_{0.17})_3$ and $FA_{0.83}MA_{0.17}Pb(I_{0.83}Br_{0.17})_3$ thin films, whose energy levels can be fully reverted to intrinsic by storage in vacuum. In contrast, purely inorganic $CsPbI_{1.8}Br_{1.2}$ thin films did not exhibit a change in the E_F position upon oxygen exposure. Oxygen, however, can passivate metallic lead-related surface states of $CsPbI_{1.8}Br_{1.2}$.

II. METHODS

A. Sample preparation

Indium-tin-oxide (ITO)-coated glass substrates were cleaned by ultrasonication sequentially with detergent, ethanol, and DI water. The wet-cleaned ITO substrates were exposed to UV–ozone for 15 min before subsequent deposition of various organic films to vary the work function. Hexaazatriphenylenehexacarbonitrile (HAT-CN; Novaled) was spin-coated from 10 mg/ml acetone solution onto the ITO substrates at 4000 rpm for 30 s. Two different formulations of poly(3,4-ethylenedioxythiophene) polystyrene sulfonate, i.e., HIL 1.3 (H. C. Starck GmbH, Φ_{sub}: 5.9 eV) and PEDOT:PSS (AI 4083, Heraeus, Φ_{sub}: 5.07 and 4.75 eV), were spin-coated from aqueous dispersion onto the ITO substrates with two-step rates at 500 rpm for 5 s and 2500 rpm for 25 s. The PEDOT:PSS films were annealed in air and a N_2-filled glove box, respectively.[31] For the uvo-PTAA substrates (Φ_{sub}: 4.68 eV), poly[bis(4-phenyl)(2,5,6-trimethylphenyl)amine] (PTAA; Sigma-Aldrich) solution was prepared at a concentration of 2 mg/ml in toluene and spin-coated onto the ITO substrates at 6000 rpm for 30 s, which was subsequently annealed at 100 °C for 10 min. The PTAA film was treated with UV–ozone for 30 s before perovskite deposition. For the PEIE substrates (Φ_{sub}: 3.85 eV), PEIE solution was prepared from poly(ethyleneimine) (Sigma-Aldrich) in 2-methoxyethanol at a concentration of 0.4 wt. %. The films were annealed at 110 °C for 10 min. For the PEIE-BuOH substrates (Φ_{sub}: 3.44 eV), PEIE solution was prepared in anhydrous butanol at a concentration of 0.4 wt. %.[31]

The $Cs_{0.05}(FA_{0.83}MA_{0.17})_{0.95}Pb(I_{0.83}Br_{0.17})_3$, $FA_{0.83}MA_{0.17}Pb(I_{0.83}Br_{0.17})_3$, and $CsPbI_{1.8}Br_{1.2}$ precursor solutions were prepared according to Refs. 10, 32, and 33. Briefly, the $Cs_{0.05}(FA_{0.83}MA_{0.17})_{0.95}Pb(I_{0.83}Br_{0.17})_3$ and $FA_{0.83}MA_{0.17}Pb(I_{0.83}Br_{0.17})_3$ precursor solutions were spin-coated at 4000 rpm for 30 s onto the substrates. 0.2 ml of ethyl acetate was dropped onto the perovskite intermediate phase film at a delay time of 8 s after the start of the spin-coating. Then, the intermediate phase perovskite films were annealed at 100 °C for 10 min. The $CsPbI_{1.8}Br_{1.2}$ precursor solution was spin-coated with two-step rates at 1000 rpm for 5 s and 3000 rpm for 40 s. The intermediate phase perovskite films were then annealed successively with three steps at 50 °C for 2 min, 100 °C for 1 min, and 160 °C for 10 min.[10] All perovskite films were fabricated in a N_2-filled glove box and directly transferred to the vacuum chamber for photoemission measurements without air exposure.

B. Photoelectron spectroscopy

Ultraviolet photoelectron spectroscopy (UPS) measurements were conducted using a SPECS PHOIBOS 100 hemispherical analyzer. As an excitation source, a monochromatized helium discharge lamp (21.22 eV) was used and a sample bias of −10 V was applied to acquire the secondary cutoff spectra. The base pressure of the analysis chamber was maintained below 5.0×10^{-10} mbar. Oxygen exposure experiments were conducted in a load-lock chamber at an O_2 pressure of 2.0×10^2 mbar, equivalent to the oxygen partial pressure in ambient conditions. For vacuum exposure, the samples were stored in the ultrahigh vacuum (UHV; base pressure: 5.0×10^{-10} mbar) chamber. Sample illumination was done using a white halogen lamp (Solux, 50 W, daylight rendering spectrum; intensity equivalent to 1.5 sun).

III. RESULTS AND DISCUSSION

A. Substrate-dependent E_F of intrinsic mixed perovskite films

To investigate the relation between E_F and Φ_{sub}, various substrates were employed with Φ_{sub} ranging from 3.5 to 5.8 eV. The work function of the mixed perovskite thin films (Φ) and the binding energy of the valence band maximum (E_{VBM}) with respect to E_F and Φ_{sub} were determined from UPS measurements (raw data are shown in Figs. S1–S2 of the supplementary material). It is noted that all E_{VBM} values were obtained by plotting the photoemission signal on a logarithmic intensity scale due to the relatively low density of states at the valence band onset of the perovskites.[8,34] The Φ and E_{VBM} values of the three mixed perovskites in dependence on Φ_{sub} are summarized in Fig. 1. From Fig. 1(a), we observe that for the Φ_{sub} values of 4.7 and 5.05 eV, the Φ value of $Cs_{0.05}(FA_{0.83}MA_{0.17})_{0.95}Pb(I_{0.83}Br_{0.17})_3$ (hereafter abbreviated as CsFAMA) films is the same as Φ_{sub}, indicating vacuum level alignment at the perovskite/substrate interface. In contrast, CsFAMA films deposited onto the substrates with the highest and lowest Φ_{sub} values exhibit a Φ value that significantly changed compared to Φ_{sub}, suggesting interfacial charge transfer instead of vacuum level alignment. The same trend is also observed for $(FA_{0.83}MA_{0.17})_{0.95}Pb(I_{0.83}Br_{0.17})_3$ (hereafter abbreviated as FAMA) and $CsPbI_{1.8}Br_{1.2}$ thin films, as observable in Figs. 1(b) and 1(c). This behavior of Φ vs Φ_{sub} is reminiscent of the transition between the vacuum level alignment regime (Schottky–Mott limit) and the E_F-pinning regimes at the frontier occupied and unoccupied energy levels, as described for organic semiconductors.[30] These three regimes are characterized by slopes of ≈1 [vacuum level alignment, denoted as (ii) in Fig. 1] and ≈0 [E_F-pinning, denoted as (i) and (iii) in Fig. 1], resulting in the so-called "Z-curve,"[30] which we added tentatively as dashed lines in the plots of Fig. 1, according to the observed trends. From this procedure, we can estimate the critical Φ_{sub} values at which E_F-pinning, and thus interfacial charge transfer to reach electronic equilibrium, sets in, termed Φ^- and Φ^+ for pinning at the conduction and valence band edges, respectively. We thus find the corresponding Φ^-/Φ^+ values for CsFAMA (4.14 eV/5.14 eV), FAMA (4.25 eV/5.04 eV), and $CsPbI_{1.8}Br_{1.2}$ (4.02 eV/5.15 eV).

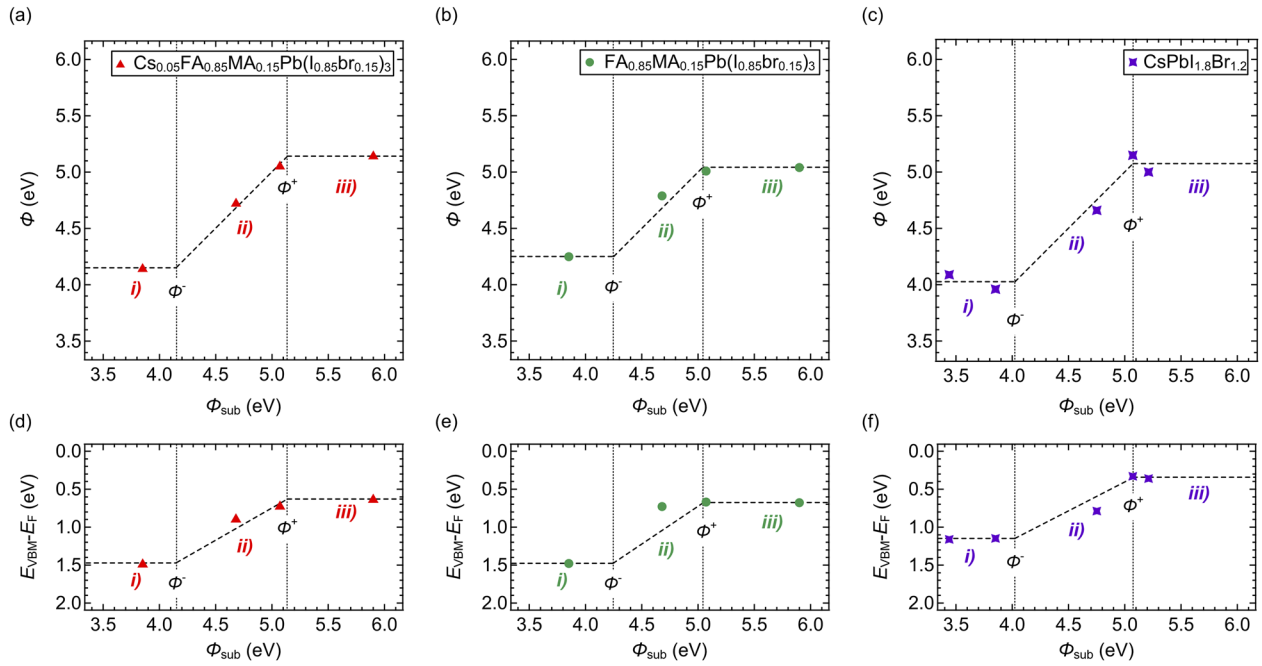

FIG. 1. Summary of the sample work function (Φ, top row) and valence band maxima ($E_{VBM} - E_F$, bottom row) of (a) and (d) $Cs_{0.05}(FA_{0.83}MA_{0.17})_{0.95}Pb(I_{0.83}Br_{0.17})_3$, (b) and (e) $FA_{0.83}MA_{0.17}Pb(I_{0.83}Br_{0.17})_3$, and (c) and (f) $CsPbI_{1.8}Br_{1.2}$ as a function of substrate work function (Φ_{sub}). Regions marked (i) and (iii) correspond to the E_F-pinning regime at the conduction and valence band edges, respectively, and (ii) indicates the vacuum level alignment regime.

For the transition between regimes (i), (ii), and (iii), the dependence of E_{VBM} on Φ_{sub} should exhibit the same slopes as Φ, which is also indicated by dashed lines in Figs. 1(d)–1(f), and yields—overall—satisfactory agreement with the experimental data for the three MHPs. Across the Φ_{sub} values studied, the E_{VBM} value of CsFAMA exhibits a total shift from 1.49 to 0.63 eV. Because E_{VBM} and Φ shift essentially in parallel, the ionization energy (IE) of all CsFAMA films is nearly constant within a reasonable error, i.e., (5.70 ± 0.09) eV. In full analogy, E_{VBM} exhibits a change from 1.48 to 0.68 eV for FAMA and from 1.16 to 0.36 eV for $CsPbI_{1.8}Br_{1.2}$, giving rise to almost constant IE values of (5.66 ± 0.10) eV for FAMA and (5.35 ± 0.17) eV for $CsPbI_{1.8}Br_{1.2}$. It is important to stress that surface photovoltage was absent in these measurements. In a previous report, it was shown that the typical UV light intensity used to excite the photoelectrons by UPS can already induce surface photovoltage in MHPs, in addition to external visible light illumination.[35] If a sample exhibits surface photovoltage, its magnitude decreases notably with reduced UV light intensity; in contrast, samples that exhibit no surface photovoltage upon varying UV light intensities do not exhibit surface photovoltage also for visible light irradiation.[35] For all perovskite samples probed here, we did not observe shifts of the energy levels within 50 meV when reducing the UV light intensity by a factor of 100, indicating negligible surface band bending effects and thus negligible surface density of states. All these observations are consistent with the notion that the three MHPs investigated here behave like intrinsic semiconductors.

We would like to mention that the slope factor in the "Z-curve" (i.e., Schottky–Mott limit) for all MHP films is estimated to be close to one (dashed lines between Φ^- and Φ^+ in Fig. 1), which is indicative of flat band conditions within the bulk. In the case where Φ_{sub} goes beyond the critical values, e.g., 4.14 and 5.15 eV for CsFAMA, electronic equilibrium is established by interfacial charge transfer. As a consequence, E_F at the interface is then pinned right at the band edges for ideal semiconductors without states tailing into the gap. In contrast, we observe from our data that the apparent movement of E_F within the gap as a function of Φ_{sub} is smaller than the bandgap values of MHPs. For instance, for CsFAMA, the total shift of E_F by 0.86 eV due to varying Φ_{sub} values is less than the bandgap of 1.63 eV.[36] We suggest that this is due to the fact that the UPS only probes the very surface (about 1 nm) of our ~500 nm thick films. At the buried interface, the interfacial charge transfer in the E_F-pinning regime leads to band bending away from the interface. For an intrinsic semiconductor, this can occur within a few nm by several hundreds of meV, followed by essentially flat band conditions in the bulk.[37] This could well explain an E_F movement at the surface that is narrower than the bandgap of the perovskites.[37–39] In addition, the presence of gap states in the vicinity of the band edges, as reported for some MHPs,[9] could also cause pinning of E_F within the gap before reaching the band edges.[40]

B. Effect of oxygen exposure on the energy levels of mixed perovskites

The diffusion of oxygen molecules into $MAPbI_3$ is known to induce *p*-doping, but the process is fully reversible upon storage of the material in vacuum for a prolonged time.[23] To investigate whether analogous effects occur also for other MHPs, first, a

CsFAMA film deposited on a uvo-PTAA substrate (not E_F-pinned to allow for possible oxygen-induced E_F movement) was exposed to oxygen at 200 mbar (equivalent to the oxygen partial pressure in ambient air) for 1 h in a vacuum chamber (base pressure: 5×10^{-7} mbar) of the photoemission setup. As can be seen in Fig. 2, after oxygen exposure, the Φ value of CsFAMA increased from 4.72 to 5.00 eV and E_{VBM} shifted completely in parallel from 0.90 to 0.62 eV; thus, the IE remained constant. Apparently, oxygen induced an E_F shift that is indicative of p-type doping. Subsequently, the oxygen exposed sample was stored in UHV (base pressure: 5.0×10^{-10} mbar) over an extended period and re-measured by UPS after 23 and 60 h of UHV storage. After 23 h, Φ and E_{VBM} shifted toward their original values, and after 60 h, the energy levels of the CsFAMA film returned entirely to their values before oxygen exposure. The complete reversibility of p-doping (oxygen exposure) and de-doping (vacuum storage) parallels the observations made earlier for $MAPbI_3$,[23] thus suggesting that oxygen molecules can readily diffuse through the CsFAMA bulk. The same reversible p-doping phenomenon by oxygen was also observed for FAMA (see Fig. S3 in the supplementary material), only of smaller magnitude. It is noted that surface photovoltage was not observed for oxygen exposed samples (variation of UV excitation intensity by ~100-fold), excluding surface band bending only due to surface-adsorbed oxygen. In addition, the rather prolonged restoring time under UHV further supports a bulk p-doping process. Szemjonov *et al.* also reported oxygen-induced Φ changes in CsFAMA films by Kelvin probe measurements and with additional theoretical modeling suggested p-doping by oxygen as a cause.[41] Here, we provide direct evidence for p-doping without any possible influence of surface dipoles, as we determine both Φ and E_{VBM} on extended timescales. The mechanism underlying the oxygen-induced p-doping is likely to be similar to the mechanistic views presented earlier.[23,41] There, it was found that O_2 interstitials are essentially electronically inactive. However, an I vacancy introduces a state close to the conduction band minimum, and when O_2 occupies that vacancy, an energy level close to the valence band maximum is established, thus explaining a change in the material from n-type to p-type. Yet, this model needs to be reconciled with our observation that the MHP films appear rather intrinsic before oxygen exposure. This could be explained by the initial presence of I vacancies (n-type) and I interstitials (p-type) that balance their doping effects so that overall the samples appear intrinsic before oxygen exposure.

In contrast to the behavior of both CsFAMA and FAMA, all-inorganic $CsPbI_{1.8}Br_{1.2}$ exhibited almost constant Φ (3.96–3.91 eV) and E_{VBM} (1.15–1.14 eV) values even after 3 h of oxygen exposure (see Fig. 3), showing that p-doping does not occur. On the one hand, this could indicate that oxygen diffusion through the inorganic perovskite is significantly slower than through MHPs containing organic cations, where the temperature-induced motion of the bulky organic molecules could provide an energy landscape favorable for oxygen transport. On the other hand, it was suggested that the p-doping process by oxygen in $MAPbI_3$ is predominantly caused by oxygen molecules substituting halogen vacancies.[23] Therefore, inorganic perovskite films might feature fewer halogen vacancies and explain the absence of oxygen-induced p-doping despite possible oxygen diffusion.

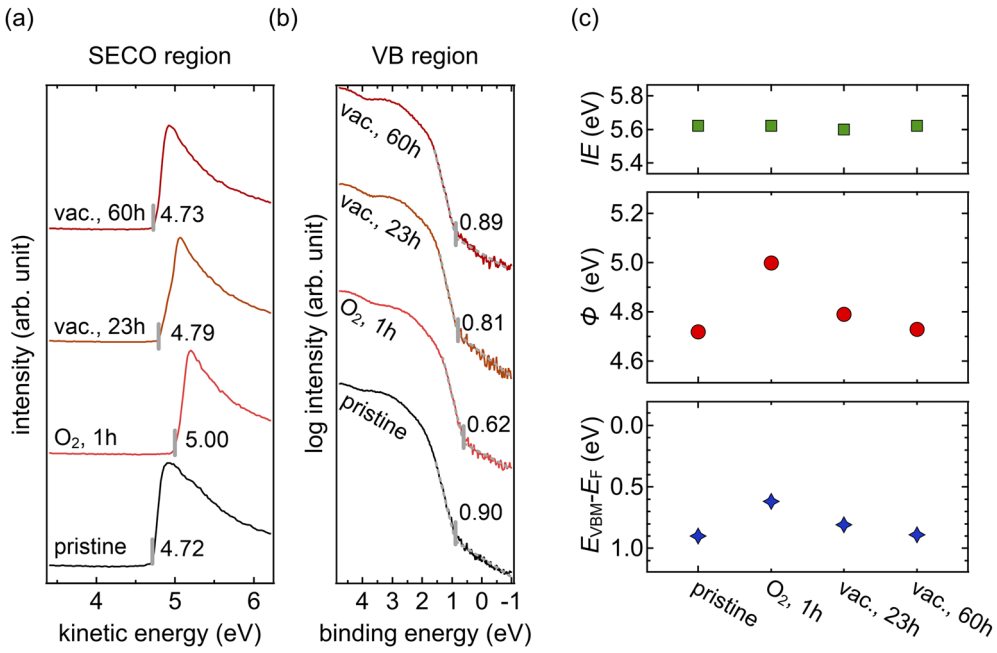

FIG. 2. UPS spectra of the (a) SECO and the (b) valence region of a $Cs_{0.05}(FA_{0.83}MA_{0.17})_{0.95}Pb(I_{0.83}Br_{0.17})_3$ film on a uvo-PTAA substrate before and after successive oxygen and UHV exposure and (c) key electronic parameters extracted from the UPS data.

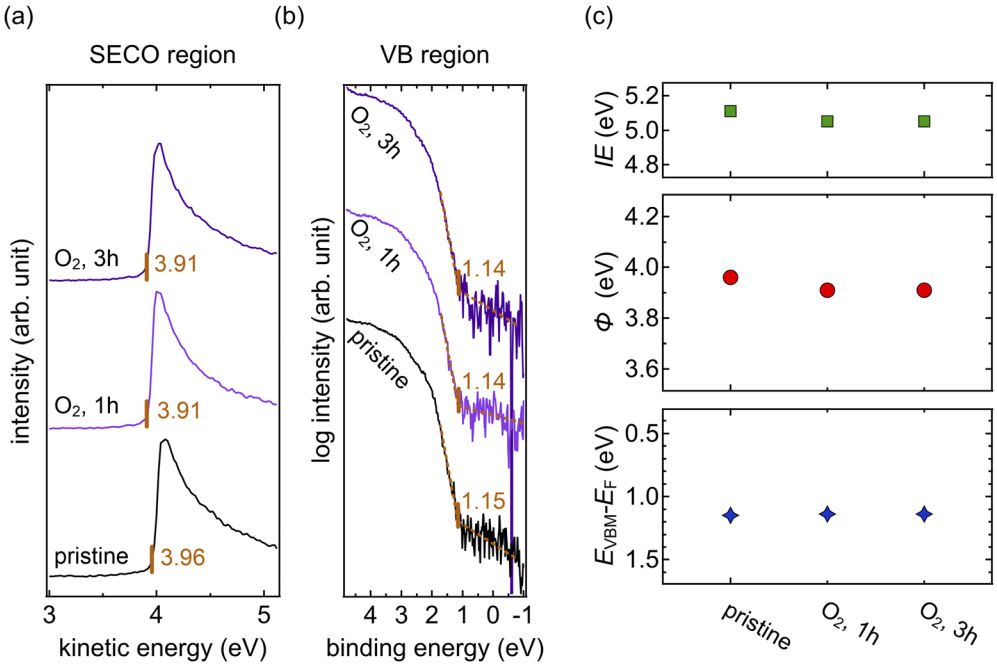

FIG. 3. UPS spectra of the (a) SECO and the (b) valence region of the $CsPbI_{1.8}Br_{1.2}$ inorganic perovskite film on a PEIE substrate before and after successive oxygen exposure and (c) key electronic parameters extracted from the UPS data.

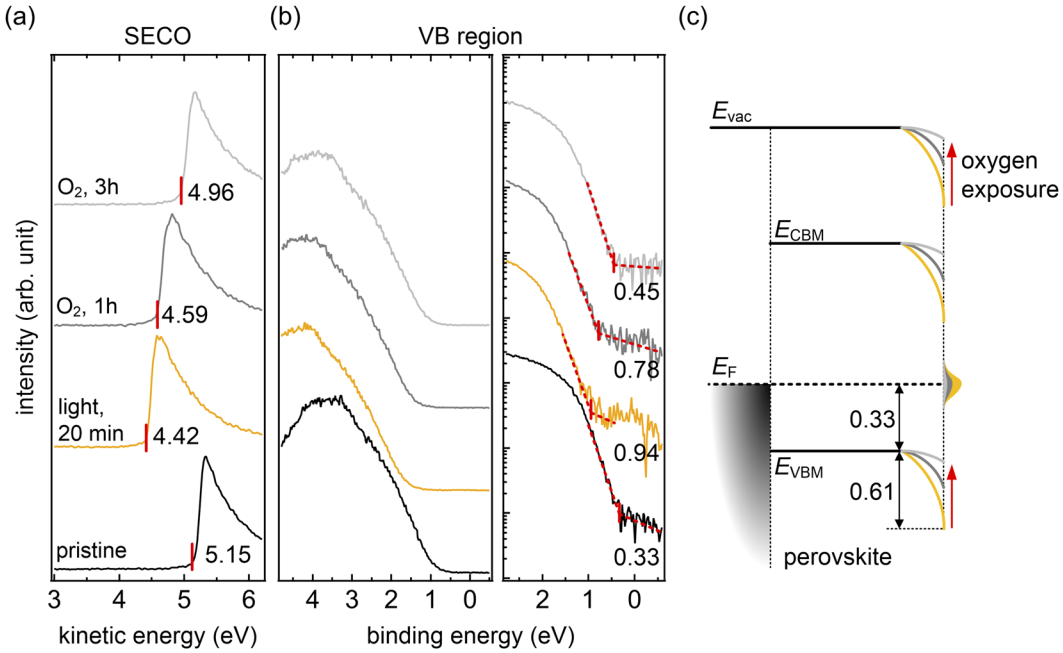

FIG. 4. UPS spectra of the (a) SECO and the (b) valence region of a $CsPbI_{1.8}Br_{1.2}$/PEDOT:PSS sample treated consecutively by white light illumination (intensity equivalent to 1.5 sun) under UHV and oxygen exposure. (c) Schematic energy level diagram derived from the UPS data, including the Pb^0-related (white light induced) surface states near E_F.

C. Impact of oxygen exposure on the surface states of $CsPbI_{1.8}Br_{1.2}$

Recent investigations on the all-inorganic perovskite $CsPbBr_3$ revealed an enhancement of the photoluminescence yield upon oxygen exposure,[42] which was attributed to defect passivation on the surface, in line with other studies.[39,43–45] To further investigate this issue, a $CsPbI_{1.8}Br_{1.2}$ film was exposed to the white light (intensity equivalent to ~1.5 sun) for 20 min under UHV, which is expected to create surface halide vacancies and subsequently generate metallic Pb^0-related surface states.[35,46] As seen in Fig. 4 (yellow curves), this treatment indeed leads to a finite density of states at and just below E_F, which is absent for the pristine film. These states are assigned to stem from the Pb^0 surface defects of *n*-type nature, in analogy to earlier studies.[35,46] Accordingly, Φ shifts from 5.15 to 4.42 eV and E_{VBM} from 0.33 to 0.94 eV. These shifts are clear signs of downward surface band bending due to donor-type surface states. The sample was then exposed to oxygen for up to 3 h, and Φ and E_{VBM} recovered almost their initial values. This is accompanied by a significant reduction of surface state density in the vicinity of E_F, evidencing the electronic passivation by oxygen. Furthermore, to show that the surface passivation effect does not depend on the substrate, we investigated $CsPbI_{1.8}Br_{1.2}$ deposited onto a HAT-CN substrate (see Fig. S4 in the supplementary material) and observed the same trends of light-induced surface states and their disappearance after oxygen exposure.

IV. CONCLUSION

The electronic properties of mixed-cation/mixed-halide metal halide perovskites, i.e., $Cs_{0.05}(FA_{0.83}MA_{0.17})_{0.95}Pb(I_{0.83}Br_{0.17})_3$, $FA_{0.83}MA_{0.17}Pb(I_{0.83}Br_{0.17})_3$, and $CsPbI_{1.8}Br_{1.2}$, deposited onto substrates with widely varying work functions were studied by UPS. The dependencies of the perovskite work function and the position of E_F in the gap on Φ_{sub} show the behavior expected for an intrinsic semiconductor, with a regime following the Schottky–Mott limit (vacuum level alignment) and regimes where E_F-pinning close to the conduction/valence band edges occurs. This, however, is only the case for CsFAMA and FAMA thin films that were not exposed to oxygen. Upon oxygen exposure (for 10 min), these two materials become strongly *p*-doped due to oxygen diffusion into the bulk, where oxygen molecules most likely occupy halogen vacancies. The diffusion and p-doping are fully reversible, and the intrinsic material properties can be restored by long-term (10 h) storage in UHV. In contrast, the electronic properties of all-inorganic $CsPbI_{1.8}Br_{1.2}$ are not affected by oxygen exposure for up to 3 h. We propose that either the diffusion of oxygen through $CsPbI_{1.8}Br_{1.2}$ is significantly lower than through the organic/inorganic perovskites or it does not feature a large density of native halogen vacancies. However, oxygen exposure is found to passivate (light-induced) metallic lead-related surface states of $CsPbI_{1.8}Br_{1.2}$. These findings provide a comprehensive understanding of the electronic properties of a range of contemporary MHPs, particularly dependence of oxygen exposure, and emphasize the importance of meticulous control and reporting of the sample environment during studies on MHPs.

SUPPLEMENTARY MATERIAL

See the supplementary material for ultraviolet photoelectron spectroscopy data.

ACKNOWLEDGMENTS

This study was supported by the Deutsche Forschungsgemeinschaft (DFG, German Research Foundation, Grant Nos. 182087777-SFB951 and 423749265-SPP2196 "SURPRISE").

The authors declare no competing financial interest.

DATA AVAILABILITY

The data that support the findings of this study are available from the corresponding author upon reasonable request.

REFERENCES

[1] J. Huang, Y. Yuan, Y. Shao, and Y. Yan, Nat. Rev. Mater. **2**, 17042 (2017).
[2] H. Jin, E. Debroye, M. Keshavarz, I. G. Scheblykin, M. B. J. Roeffaers, J. Hofkens, and J. A. Steele, Mater. Horiz. **7**, 397 (2020).
[3] P. Schulz, D. Cahen, and A. Kahn, Chem. Rev. **119**, 3349 (2019).
[4] D. W. Dequilettes, K. Frohna, D. Emin, T. Kirchartz, V. Bulovic, D. S. Ginger, and S. D. Stranks, Chem. Rev. **119**, 11007 (2019).
[5] L. Qiu, S. He, L. K. Ono, and Y. Qi, Adv. Energy Mater. **10**, 1902726 (2020).
[6] D. Niesner, APL Mater. **8**, 090704 (2020).
[7] I. Lange, J. C. Blakesley, J. Frisch, A. Vollmer, N. Koch, and D. Neher, Phys. Rev. Lett. **106**, 216402 (2011).
[8] F. Zu, P. Amsalem, D. A. Egger, R. Wang, C. M. Wolff, H. Fang, M. A. Loi, D. Neher, L. Kronik, S. Duhm, and N. Koch, J. Phys. Chem. Lett. **10**, 601 (2019).
[9] F. Zhang, J. C. Hamill, Y. L. Loo, and A. Kahn, Adv. Mater. **32**, 2003482 (2020).
[10] Q. Wang, F. Zu, P. Caprioglio, C. M. Wolff, M. Stolterfoht, M. Li, S.-H. Turren-Cruz, N. Koch, D. Neher, and A. Abate, ACS Energy Lett. **5**, 2343 (2020).
[11] M. Ralaiarisoa, I. Salzmann, F. S. Zu, and N. Koch, Adv. Electron. Mater. **4**, 1800307 (2018).
[12] C. M. Wolff, P. Caprioglio, M. Stolterfoht, and D. Neher, Adv. Mater. **31**, 1902762 (2019).
[13] N. K. Noel, S. N. Habisreutinger, A. Pellaroque, F. Pulvirenti, B. Wenger, F. Zhang, Y.-H. Lin, O. G. Reid, J. Leisen, Y. Zhang, S. Barlow, S. R. Marder, A. Kahn, H. J. Snaith, C. B. Arnold, and B. P. Rand, Energy Environ. Sci. **12**, 3063 (2019).
[14] D. Shin, D. Kang, J. Jeong, S. Park, M. Kim, H. Lee, and Y. Yi, J. Phys. Chem. Lett. **8**, 5423 (2017).
[15] D. Shin, D. Kang, J.-B. Lee, J.-H. Ahn, I.-W. Cho, M.-Y. Ryu, S. W. Cho, N. E. Jung, H. Lee, and Y. Yi, ACS Appl. Mater. Interfaces **11**, 17028 (2019).
[16] C. M. Wolff, F. Zu, A. Paulke, L. P. Toro, N. Koch, and D. Neher, Adv. Mater. **29**, 1700159 (2017).
[17] A. Zohar, M. Kulbak, I. Levine, G. Hodes, A. Kahn, and D. Cahen, ACS Energy Lett. **4**, 1 (2019).
[18] S. Olthof, APL Mater. **4**, 091502 (2016).
[19] P. Schulz, L. L. Whittaker-Brooks, B. A. MacLeod, D. C. Olson, Y.-L. Loo, and A. Kahn, Adv. Mater. Interfaces **2**, 1400532 (2015).
[20] M. Oehzelt, K. Akaike, N. Koch, and G. Heimel, Sci. Adv. **1**, e1501127 (2015).
[21] J. Emara, T. Schnier, N. Pourdavoud, T. Riedl, K. Meerholz, and S. Olthof, Adv. Mater. **28**, 553 (2016).
[22] N. K. Noel, S. N. Habisreutinger, B. Wenger, Y. H. Lin, F. Zhang, J. B. Patel, A. Kahn, M. B. Johnston, and H. J. Snaith, Adv. Energy Mater. **10**, 1903231 (2020).
[23] D. Shin, F. Zu, A. V. Cohen, Y. Yi, L. Kronik, and N. Koch, Adv. Mater. **33**, 2100211 (2021).
[24] C. Yi, J. Luo, S. Meloni, A. Boziki, N. Ashari-Astani, C. Grätzel, S. M. Zakeeruddin, U. Röthlisberger, and M. Grätzel, Energy Environ. Sci. **9**, 656 (2016).
[25] L. Zhang, X. Yang, Q. Jiang, P. Wang, Z. Yin, X. Zhang, H. Tan, Y. Yang, M. Wei, B. R. Sutherland, E. H. Sargent, and J. You, Nat. Commun. **8**, 15640 (2017).
[26] N. Li, Z. Zhu, C.-C. Chueh, H. Liu, B. Peng, A. Petrone, X. Li, L. Wang, and A. K.-Y. Jen, Adv. Energy Mater. **7**, 1601307 (2017).
[27] D. P. McMeekin, Z. Wang, W. Rehman, F. Pulvirenti, J. B. Patel, N. K. Noel, M. B. Johnston, S. R. Marder, L. M. Herz, and H. J. Snaith, Adv. Mater. **29**, 1607039 (2017).

[28]M. Kulbak, I. Levine, E. Barak-Kulbak, S. Gupta, A. Zohar, I. Balberg, G. Hodes, and D. Cahen, Adv. Energy Mater. **8**, 1800398 (2018).
[29]J. Endres, M. Kulbak, L. Zhao, B. P. Rand, D. Cahen, G. Hodes, and A. Kahn, J. Appl. Phys. **121**, 035304 (2017).
[30]S. Braun, W. R. Salaneck, and M. Fahlman, Adv. Mater. **21**, 1450 (2009).
[31]S. Bontapalle, A. Opitz, R. Schlesinger, S. R. Marder, S. Varughese, and N. Koch, Adv. Mater. Interfaces **7**, 2000291 (2020).
[32]M. Saliba, J.-P. Correa-Baena, C. M. Wolff, M. Stolterfoht, N. Phung, S. Albrecht, D. Neher, and A. Abate, Chem. Mater. **30**, 4193 (2018).
[33]M. Saliba, T. Matsui, J.-Y. Seo, K. Domanski, J.-P. Correa-Baena, M. K. Nazeeruddin, S. M. Zakeeruddin, W. Tress, A. Abate, A. Hagfeldt, and M. Grätzel, Energy Environ. Sci. **9**, 1989 (2016).
[34]J. Endres, D. A. Egger, M. Kulbak, R. A. Kerner, L. Zhao, S. H. Silver, G. Hodes, B. P. Rand, D. Cahen, L. Kronik, and A. Kahn, J. Phys. Chem. Lett. **7**, 2722 (2016).
[35]F. Zu, P. Amsalem, M. Ralaiarisoa, T. Schultz, R. Schlesinger, and N. Koch, ACS Appl. Mater. Interfaces **9**, 41546 (2017).
[36]F. Peña-Camargo, P. Caprioglio, F. Zu, E. Gutierrez-Partida, C. M. Wolff, K. Brinkmann, S. Albrecht, T. Riedl, N. Koch, D. Neher, and M. Stolterfoht, ACS Energy Lett. **5**, 2728 (2020).
[37]M. Oehzelt, N. Koch, and G. Heimel, Nat. Commun. **5**, 4174 (2014).
[38]W.-Q. Wu, Z. Yang, P. N. Rudd, Y. Shao, X. Dai, H. Wei, J. Zhao, Y. Fang, Q. Wang, Y. Liu, Y. Deng, X. Xiao, Y. Feng, and J. Huang, Sci. Adv. **5**, eaav8925 (2019).
[39]H.-H. Fang, S. Adjokatse, H. Wei, J. Yang, G. R. Blake, J. Huang, J. Even, and M. A. Loi, Sci. Adv. **2**, e1600534 (2016).
[40]R. Schlesinger, F. Bussolotti, J. Yang, S. Sadofev, A. Vollmer, S. Blumstengel, S. Kera, N. Ueno, and N. Koch, Phys. Rev. Mater. **3**, 074601 (2019).
[41]A. Szemjonov, K. Galkowski, M. Anaya, Z. Andaji-Garmaroudi, T. K. Baikie, S. Mackowski, I. D. Baikie, S. D. Stranks, and M. S. Islam, ACS Mater. Lett. **1**, 506 (2019).
[42]C. Rodà, A. L. Abdelhady, J. Shamsi, M. Lorenzon, V. Pinchetti, M. Gandini, F. Meinardi, L. Manna, and S. Brovelli, Nanoscale **11**, 7613 (2019).
[43]R. Brenes, D. Guo, A. Osherov, N. K. Noel, C. Eames, E. M. Hutter, S. K. Pathak, F. Niroui, R. H. Friend, M. S. Islam, H. J. Snaith, V. Bulović, T. J. Savenije, and S. D. Stranks, Joule **1**, 155 (2017).
[44]M. Anaya, J. F. Galisteo-López, M. E. Calvo, J. P. Espinós, and H. Míguez, J. Phys. Chem. Lett. **9**, 3891 (2018).
[45]D. Meggiolaro, E. Mosconi, and F. De Angelis, ACS Energy Lett. **2**, 2794 (2017).
[46]F.-S. Zu, P. Amsalem, I. Salzmann, R.-B. Wang, M. Ralaiarisoa, S. Kowarik, S. Duhm, and N. Koch, Adv. Opt. Mater. **5**, 1700139 (2017).